JOURNAL OF GEOPHYSICAL RESEARCH, VOL. 105, NO. A7, PAGES 15,689–15,698, JULY 1, 2000

Ulysses observations of sector boundaries at aphelion

J. De Keyser and M. Roth

Belgian Institute for Space Aeronomy, Brussels

R. Forsyth

The Blackett Laboratory, Imperial College, London

D. Reisenfeld

Los Alamos National Laboratory, Los Alamos, New Mexico

Abstract. We study a sample of sector boundaries observed by Ulysses near its early 1998 aphelion at 5.4 AU. We relate these sector boundaries to solar wind structure seen by Wind at 1 AU, guided by a hydrodynamic simulation. For each Ulysses sector boundary we are able to identify a corresponding 1 AU sector boundary, except when strong transients are present. Sector boundaries appear embedded in complex plasma structures that generally are in a state of pressure balance. Minimum variance analysis confirms the tangential discontinuity nature of the heliospheric current sheet (HCS) and indicates that the current sheet tends to be inclined more steeply than at 1 AU (HCS normal closer to the equatorial plane and nearly radially outward). We discuss evidence for the nonplanarity of the current sheet. Magnetic field depressions are characteristic features of the sector boundaries. We attribute them to particles that are magnetically confined inside the current sheet and that carry the diamagnetic current responsible for the large magnetic field rotation.

1. Introduction

During solar minimum conditions the inner heliosphere is dominated by the presence of coronal holes near the Sun's poles, from which open magnetic field lines emanate, and by closed magnetic field lines with their footpoints in the equatorial photosphere. Fast solar wind (750 km s^{-1}) streams out of the polar coronal holes, while the wind in the equatorial region is slower (400 km s^{-1}) [*Forsyth et al.*, 1996; *Goldstein et al.*, 1996]. The magnetic field vectors in both hemispheres are opposite and follow the Parker spiral pattern. The interface between both magnetic hemispheres is the heliospheric current sheet (HCS). Observations of the interplanetary magnetic field (IMF) from a fixed low latitude vantage point reveal successive sectors of alternating IMF polarity during each solar rotation, separated by sector boundaries (SBs), which are crossings of the HCS [*Wilcox and Ness*, 1965; *Svalgaard et al.*, 1975]. At solar minimum the HCS has a gently undulating shape and remains confined to low heliographic latitudes [*Thomas and Smith*, 1981; *Forsyth et al.*, 1996]. Because of the space and time variability of the coronal field and because of the dynamic interaction between fast and slow solar wind streams the structure of a sector boundary can be very complex. Often the neutral surface (defined as the surface where the magnetic field component along the Parker spiral vanishes) is encountered several times in rapid succession [*Behannon et al.*, 1981]. The magnetic field near sector boundaries may also deviate significantly from the Parker spiral direction. The normals to the multiply encountered neutral surfaces are aligned only grossly, a fact that has led to the suggestion that the surface is rippled [*Behannon et al.*, 1981] or that it consists of a set of deformed flux tubes [*Crooker et al.*, 1996].

The purpose of this paper is to look at HCS crossings observed by Ulysses near aphelion (January–March 1998, 5.4 AU). These observations are special in the sense that (1) Ulysses spends considerable time at low heliographic latitude only near aphelion, (2) the Wind spacecraft was an excellent 1 AU solar wind monitor, being more or less radially aligned with Ulysses during this period, and (3) at 5 AU the magnetic field is so weak that the 1 s Ulysses magnetometer time resolution results in its best spatial resolution of $\sim$1 thermal ion gyroradius in the flow direction. In section 2 we present a hydrodynamic simulation that we will use to relate HCS crossings at 1 and 5 AU. Three case studies (sections 3–5) illustrate how HCS structure is determined by the magnetic confinement of particles near and inside the current sheet. We discuss a number of indications suggesting that the HCS is not simply planar. The Wind-Ulysses comparison corroborates this interpretation and illustrates the spatial and temporal extents of this nonplanarity. We also present evidence of the occasional heating of the particles in the current layer. We conclude with a discussion of the importance of these findings for the overall state of the inner heliosphere.

Paper number 2000JA900040.
0148-0227/00/2000JA900040$09.00

2. Global Sector Structure

In order to understand the global solar wind structure during the Wind-Ulysses radial alignment period, we try to relate the observations at 1 and 5 AU. The delay between the observation of a feature by Wind and by Ulysses depends on (1) solar wind speed and radial distance, (2) the solar longitude difference between both satellites, and (3) the dynamic evolution of the solar wind. It takes 18 days for a 400 km s^{-1} wind to travel 4 AU outward. The longitude difference changes from $-50°$ to $+50°$ during this period, adding -4 to +4 days to the delay. The long traveling time from 1 to 5 AU and the corresponding dynamic evolution of the solar wind make it difficult to correlate structures observed by Wind and Ulysses. In order to guide such a correlative study we have used the observed Wind plasma density, ion temperature, and radial velocity for the period December 1997 to March 1998 as inflow boundary condition in a spherically symmetric hydrodynamic code. We have extended this code by adding the magnetic field polarity (measured as the cosine of the angle between the magnetic field vector and the outward Parker spiral direction) as a quantity that is convected with the flow. We have sampled (rather than averaged) the Wind data at a time resolution commensurate with the spatial resolution used in the simulation. The numerical dissipation of the code quickly filters out the highest frequencies in the sampled 1 AU data as the solar wind moves outward.

Figure 1 shows how the number density evolves with increasing heliocentric distance (overall scaling with r^{-2}). The magnetic field polarity is indicated here by the shading of the graph (light gray corresponds to an inward magnetic field, and dark gray corresponds to an outward field). The timescale holds for observers at the same solar longitude as Wind; in order to compare with the Ulysses observations one must account for the time shift due to the aforementioned solar longitude difference between both spacecraft. The simulation therefore allows us to correlate corresponding SBs; we will present such comparisons in the case studies below. Figure 1 shows that most SBs occur in or near interaction regions (high-density regions), as expected. Figure 1 suggests that the overall sector pattern is conserved as the solar wind expands.

Using the polarity as an indicator of latitudinal distance from the HCS and interpreting temporal changes as longitudinal variations, we can qualitatively reconstruct the HCS surface, as in Figure 2. We adopt a Harris-type field reversal across the HCS [*Harris*, 1962]: $B_{\text{spiral}}/B = \tanh(x/x_0)$. Here, $p = B_{\text{spiral}}/B$ is the relative magnitude of the magnetic field component in the spiral direction, that is, our measure p of the polarity. The latitudinal distance between the satellite (for simplicity, taken to be exactly at the equator) and the center of the HCS is $x = r\sin\theta \approx r\theta$, where r is the distance from the Sun and θ is the latitude of the HCS center. The half-width of the HCS is $x_0 = r\sin\theta_0 \approx r\theta_0$, with θ_0 the angular HCS half-thickness. So, $p \approx \tanh(\theta/\theta_0)$. Choosing θ_0 in such a way that the maximum HCS excursion is 20°-30° (the typical value from Ulysses out-of-ecliptic observations), we thus have a recipe to qualitatively infer the HCS excursion θ from the polarity p. Figure 2 clearly reveals the Parker spiral pattern. The Parker spiral angle (given by $\tan\phi_P = r\Omega_S/V_{sw}$, where Ω_S is the solar rotation rate and V_{sw} is the solar wind velocity) changes from 45° at 1 AU to 80° at 5 AU. A consequence of this tight winding of the spiral is that SBs at 5 AU are more manifest as changes in the azimuthal magnetic field than in the radial field.

Another consequence evident in Figure 2 is the increasing steepness of the HCS. Indeed, while north-south and east-west distances scale with r for a radially expanding, constant velocity wind, radial distances remain constant. Consequently, both the north-south tilt and the east-west orientation of the HCS force the HCS normal to be pointing progressively more radially outward. An additional steepening of the HCS is expected from a kinematic point of view as solar wind speed increases with latitude away from the magnetic equator [*Suess and Hildner*, 1985, Figure 2b]. To what extent this steepening is opposed by the dynamical response of the wind remains to be verified and probably depends from case to case. Statistical analysis of interaction regions (in which the HCS is embedded) suggests that their typical inclination is solar cycle dependent [*González-Esparza and Smith*, 1997].

The one-dimensional hydrodynamic approximation cannot properly account for geometrical effects and ignores the role of the magnetic field. While the magnetic pressure decreases faster than the plasma pressure as heliocentric distance increases, even at 5 AU, plasma beta frequently is below 1, so that the hydrodynamic approximation generally overestimates the amount of dynamical evolution as the existence of the magnetic field energy reservoir is ignored. Because of the one-dimensional nature of the code it is impossible to distinguish between stream interaction regions and coronal mass ejections: Both correspond to pressure pulses. Moreover, while such pulses cover a limited solid angle, they are considered omnidirectional in the simulation. In reality the pulses can expand laterally and are smoothed out faster than the hydrodynamic code predicts, explaining why the velocity profile observed by Ulysses is flatter than the simulated profile. While the hydrodynamic model is better than a purely kinematic treatment, it is obviously less sophisticated than a magnetohydrodynamic approach, such as the one used by *Pizzo et al.* [1995] for a radial alignment of IMP 6/7 with Pioneer 10 and 11 (at 1, 5.5, and 4.5 AU) at a time when the solar wind was characterized by a persistent regular sector pattern, free of strong transients. Nevertheless, the hydrodynamic code serves our purpose well, namely, that of correlating sector boundaries observed by Wind and Ulysses.

3. HCS Crossing on April 10, 1998

Figure 3 illustrates a case of typical sector structure. We consider an outward sector (dark shading) observed by Wind on March 22–24, 1998, bounded by SBs embedded in interaction regions, with fast wind in the leading part and slow wind in the trailing part of the sector [*Wilcox and Ness*, 1965]. This sector can easily be traced in the simulation and is seen by Ulysses on April 8–10, 1998. We consider the trailing SB in more detail.

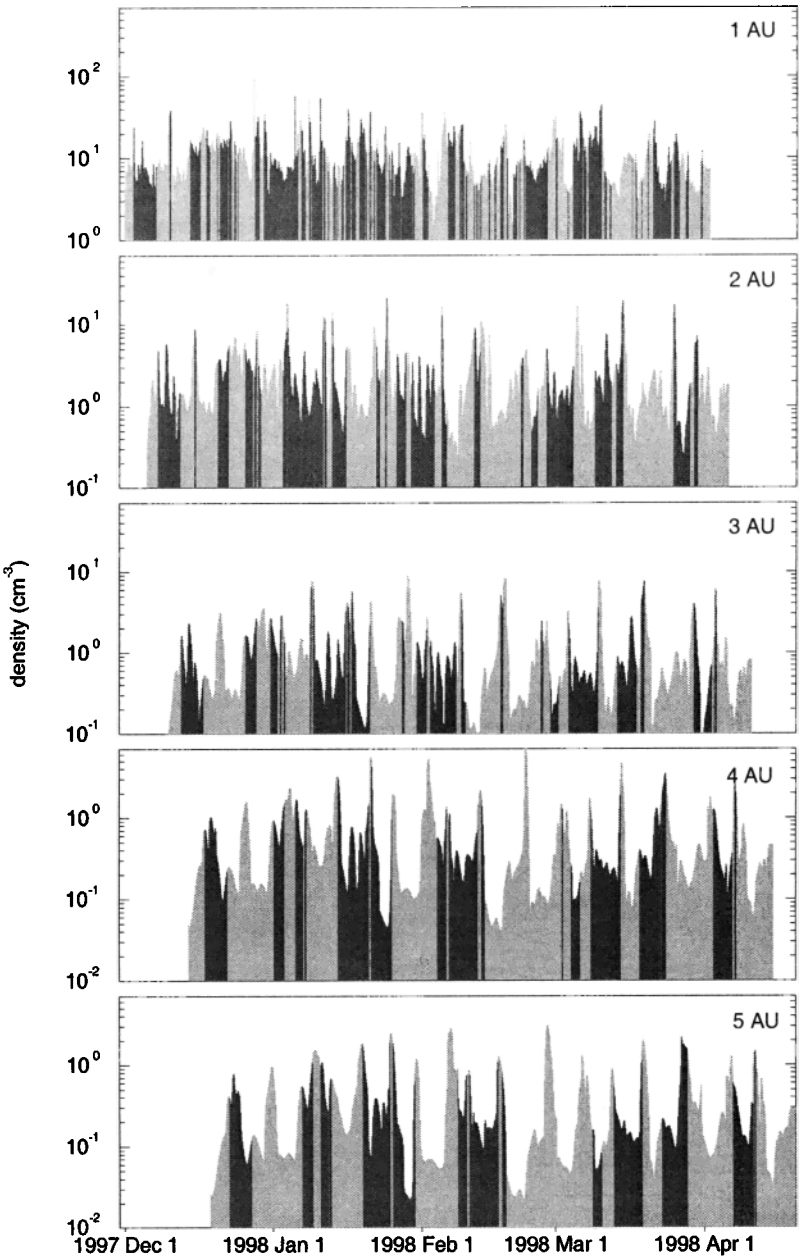

Figure 1. Results of a spherically symmetric hydrodynamic simulation of the solar wind. The input are Wind observations at 1 AU from December 1997 to March 1998. The figure shows how the number density profile changes with distance (overall scaling with r^{-2}). The time axis refers to an observer at the same solar longitude as Wind. Light gray shading indicates inward magnetic field polarity; dark shading indicates outward polarity.

A direct comparison of the Wind and Ulysses magnetic field measurements in the neighborhood of the SB is difficult as the magnetic field strength, the Parker angle, and the HCS inclination change between 1 and 5 AU. Nevertheless, we observe a strong similarity in the magnetic field profiles. This is illustrated in Figure 4, which plots the angle α between the magnetic field vector and the outward spiral direction (which includes both north-south and east-west deflections of the field with respect to the spiral orientation). In both cases there is a main SB, preceded and followed by similar minor fluctuations. We interpret these as being due to partial reentries into the curved current sheet.

Figure 5 zooms in on this SB at the trailing edge of the outward sector at 5 AU. The most natural frame to study such a transition is its minimum variance frame (MVF); B_x, B_y, and B_z denote the minimum, intermediate, and maximum magnetic field variance directions, respectively. The velocity component normal to the plane of the transition can then be used to translate time of observation into distance from the center of the sheet: that is what we have done in this and subsequent figur · Figure 5 shows a distinct heliospheric plasma sheet (HPS) signature [*Winterhalter et al.*, 1994]: a density enhancement and magnetic field depression, 1.5 × 10^6 km or 3000 ion gyroradii wide, in which

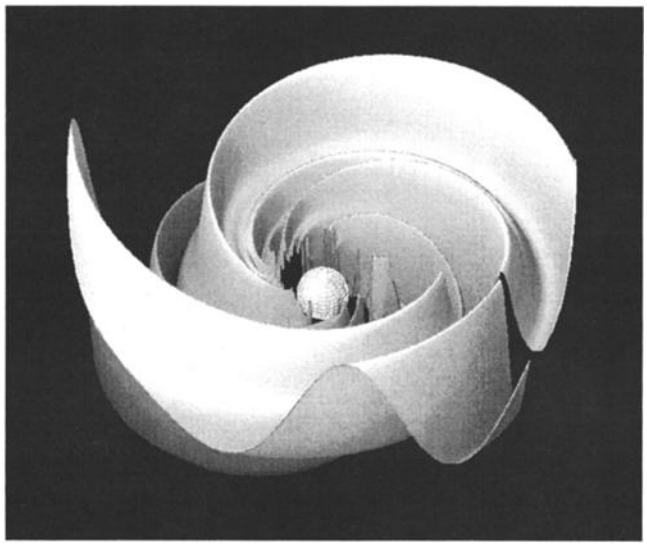

Figure 2. Qualitative reconstruction of the HCS surface between 1 and 5 AU. The plot presents the simulation results for February 1998. Temporal changes are interpreted as longitudinal variations, and the latitudinal excursion of the HCS is assumed proportional to the cosine of the angle between the magnetic field vector and the Parker spiral direction, with an arbitrary scaling factor (chosen so as to obtain realistic latitudinal HCS excursions). The "cut" in the plotted surface separates data one solar rotation apart; the degree to which the surface matches across the cut indicates the overall persistence of solar conditions during this rotation. Note that the size of the solar sphere is exaggerated.

the SB is embedded. On this scale the layer appears planar, although there are some B_x variations; the normal to the layer is inclined only 25° from the antisunward direction (the inclination at 1 AU is similar). The transition consists of subsequent "steps." There appears to be pressure balance (all data were first interpolated to the time resolution of the ion data in order to compute the thermal and magnetic pressures; isotropic temperatures were used rather than perpendicular temperatures); the lack of electron data prohibits us to verify this in more detail.

Zooming in further on the structure of this SB, we find that the largest magnetic field rotation is concentrated in the single thin sheet shown in Figure 6. Pressure balance, the zero normal MVF magnetic field, and the different solar wind plasma parameters on either side of the structure suggest that the SB is a tangential discontinuity (TD), a (locally) impermeable sheet interfacing two distinct plasmas. This is consistent with the findings of *Winterhalter et al.* [1994] regarding the HPS and the statistical studies of *Klein and Burlaga* [1980], *Behannon et al.* [1981], *Villante and Bruno* [1982], and *Lepping et al.* [1996] regarding the HCS. The magnetic field data (1 s time resolution) show a polarity reversal (160° magnetic field rotation) accompanied by a magnetic field depression; the plasma data time resolution is insufficient to resolve the corresponding plasma pressure enhancement that should be there if pressure balance is satisfied. The polarity reversal takes ~10 s, corresponding to a thickness of 4000 km or only 15 ion gyroradii.

4. HCS Crossing on February 27, 1998

On February 1–13, 1998, Wind observes a very dynamic solar wind (see Figure 7): a magnetic cloud (February 4–5, 1998), a broad interaction region containing several SBs, and a fast wind stream (up to 600 km s^{-1}). The hydrodynamic simulation fails to model the evolution of the solar wind in this situation as it cannot account for the magnetic cloud geometry and as it ignores the magnetic pressure associated

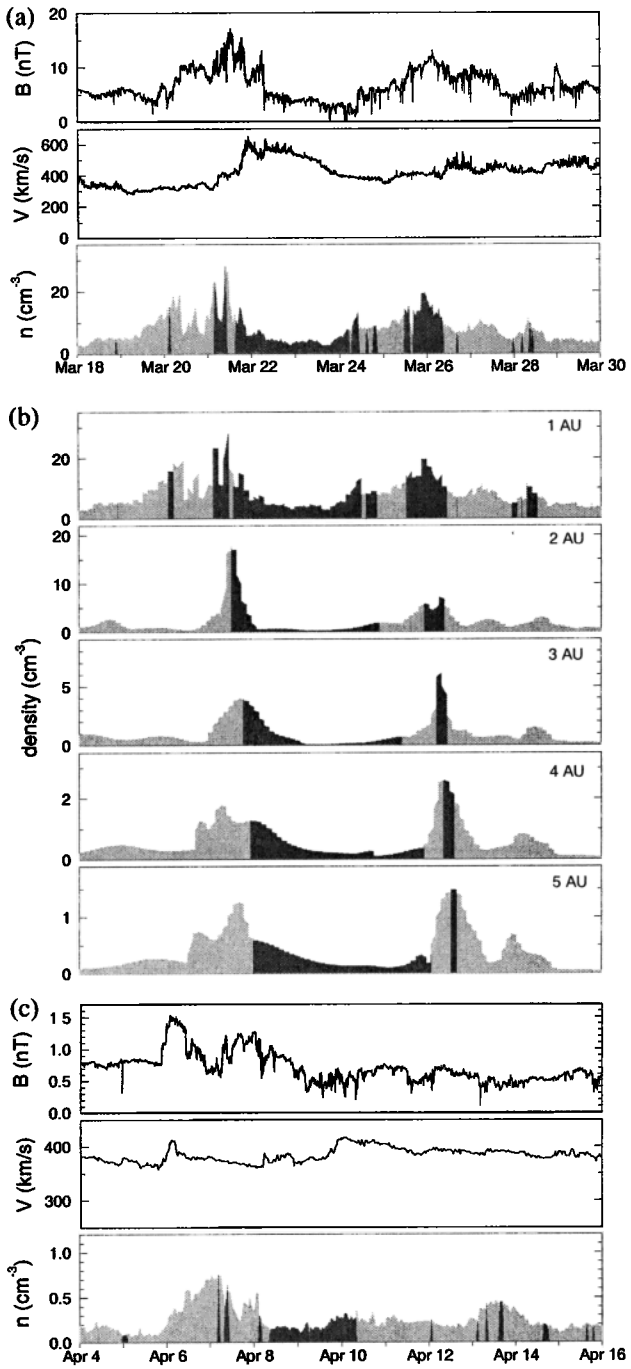

Figure 3. Evolution of an outward sector from 1 to 5 AU. (a) Wind observations at 1 AU. (b) Hydrodynamic simulation between 1 and 5 AU. (c) Ulysses observations at 5 AU. Light gray shading indicates inward magnetic field polarity; dark shading indicates outward polarity.

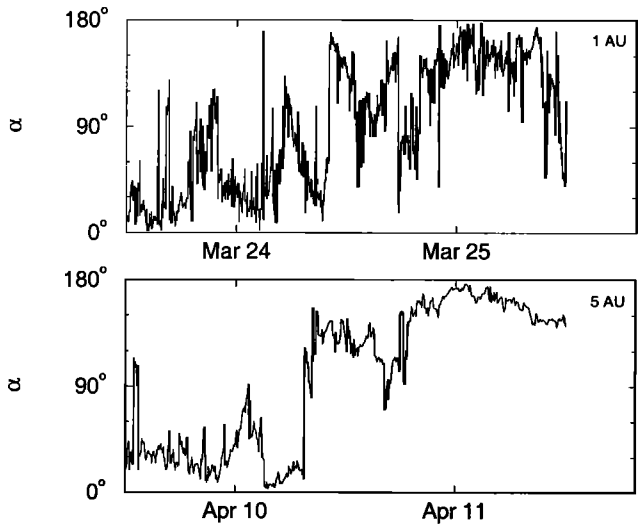

Figure 4. Comparison of the magnetic field observed by Wind (1 AU) and Ulysses (5 AU). In order to allow a comparison that is independent of the changing spiral angle and the magnetic field magnitude, we plot the angle α between the magnetic field vector and the outward Parker spiral direction.

with the cloud. The magnetic field at 1 AU is characterized by the flux rope structure typical of a magnetic cloud. There is no clear Wind counterpart for the SB that we observe in the Ulysses data on February 27, 1998. The dissimilarity between the sector structure at 1 and 5 AU may be only apparent, as the magnetic field deviates in either case significantly from the Parker spiral; the concept of "polarity" therefore

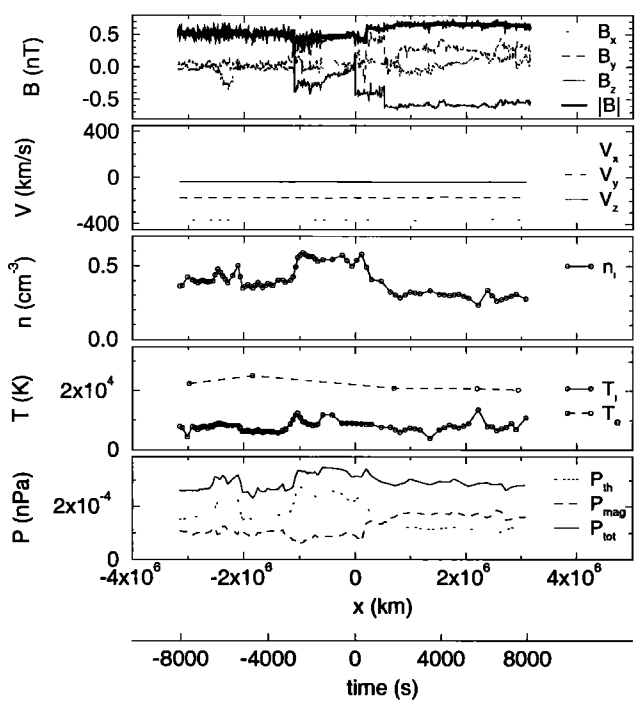

Figure 5. Context of the sector boundary observed by Ulysses on April 10, 1998. Magnetic field and solar wind velocity are shown in the minimum variance frame. The horizontal axes give the time elapsed since observation of the center of the structure and the corresponding distance.

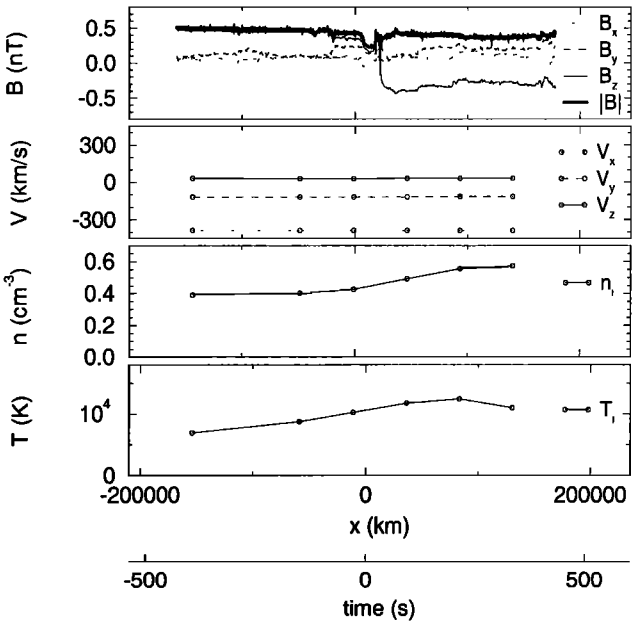

Figure 6. Sector boundary observed by Ulysses on April 10, 1998. Magnetic field and solar wind velocity are shown in the minimum variance frame. The horizontal axes give the time elapsed since observation of the center of the structure and the corresponding distance.

becomes, to some degree, irrelevant. It is not surprising that the solar wind no longer can be regarded as a medium with only two polarization states when large transient phenomena are present.

Zooming in on this transition, Figure 8 plots the Ulysses magnetic field and plasma observations in the MVF. The structure shows repeated magnetic field reversals in a wide layer ($\sim 10^7$ km or $\sim 10^5$ ion gyroradii) that is more or less planar (normal field constant and zero) and inclined with an angle of 45° to the radial direction. The layer separates regions of different density and temperature, with a tangential flow shear of a few tens of kilometers. While the total pressure remains essentially constant, there is a density peak that coincides with a region of strongly reduced magnetic field (for a discussion of the preferential occurrence of magnetic holes near the HCS, see *Klein and Burlaga* [1980]). Consequently, plasma beta (not shown) is high there ($\beta > 100$); this region can be identified as the heliospheric plasma sheet.

Figure 9a focuses on the main SB, that is, the only complete field reversal (the rightmost transition embedded in the HPS in Figure 8). The magnetic field (60 s resolution) rotates over 165° in a few minutes, corresponding to a thickness of 10^5 km or 300 ion gyroradii. The transition is associated with a magnetic field depression and small enhancements in plasma density and temperature; pressure balance is probably satisfied on this shorter distance scale as well. Note that the velocity distributions in the current layer may no longer be Maxwellian, rendering the determination of plasma density and temperature difficult. In Figure 9b we show a simulation of this transition using an equilibrium TD model [*Roth et al.*, 1996], in which electron and proton populations inside the layer drift relative to each other

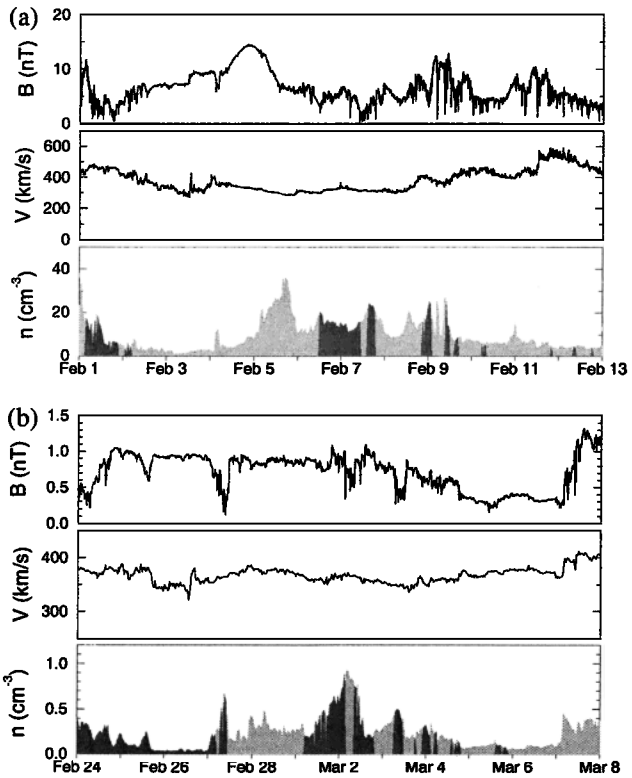

Figure 7. Solar wind evolution from 1 to 5 AU near a magnetic cloud. (a) Wind observations at 1 AU. (b) Ulysses observations at 5 AU. Light gray shading indicates inward magnetic field polarity; dark shading indicates outward polarity.

with velocities <1 km s^{-1}, implying bulk flow variations <0.2 km s^{-1}: Small drifts are sufficient to generate the diamagnetic current that causes the magnetic field to rotate.

5. HCS Crossing on January 7–8, 1998

Wind observations on December 13–25, 1997, show a continuously high-density region, in which several sectors are embedded (Figure 10). The wind is slow; solar wind speed varies from 295 km s^{-1} to 320 km s^{-1} on December 18, and somewhat faster wind is observed on December 24. The long duration of submersion in high-density wind, the repeated encounters with sectors of alternating polarity, and the absence of fast flows and distinct interaction regions suggest that Wind remained close to the undulating HCS surface throughout the entire time period. Ulysses observes a shock at the front of a first compression region on January 9, 1998, and a minor compression on January 15.

We have compared the magnetic field observations for the outward sector (dark shading) seen by Wind on December 14–17, 1997, and by Ulysses on January 6–8, 1998. The large-scale structure of the magnetic field in the sector and its boundaries are quite similar, as illustrated by the plots of the angle α between magnetic field and spiral direction (both north-south and east-west deflection) in Figure 11. This similarity implies that the large-scale curvature of the HCS is a persistent feature. While at 1 AU the current sheet is inclined 45° with respect to the radial direction, it is nearly perpendicular at 5 AU.

We focus on the SB at the end of this sector. Figure 12 shows how this transition is situated at 5 AU in a HPS structure 8 × 10^6 km across. Magnetic and plasma pressure are anticorrelated as required by pressure balance. Inside the HPS both plasma density and temperature are enhanced (no electron data are available; ion and electron temperatures were taken equal for estimating the plasma pressure). We find strong ULF fluctuations inside the HPS, most pronounced in the B_T component (bottom plot of Figure 12).

The main transition is shown in Figure 13. It is about 400,000 km or 1300 ion gyroradii wide; slight density and temperature increases and a small magnetic field reduction characterize the transition. The magnetic field reversal is not monotonous, with the major part of the field reversal occurring on a timescale of 50 s, corresponding to tens of ion gyroradii. Figure 14 shows the magnetic field hodogram. It is remarkable to see how the tangential magnetic field components change back and forth along essentially the same curve in the hodogram. This behavior is unlikely if the HCS is a sandwich structure of several separate current layers. The only plausible hypothesis is that Ulysses is actually traversing a single transition, while repeatedly moving back and forth inside it (as in multiple magnetopause crossings [*Hubert et al.*, 1998]) in a geometry like that sketched in Figure 15, where the HCS is "folded" or "rippled." Note that in such a geometry the MVF would indicate that the current sheet is perpendicular to the flow direction, while the overall surface in reality may be only slightly inclined to the flow di-

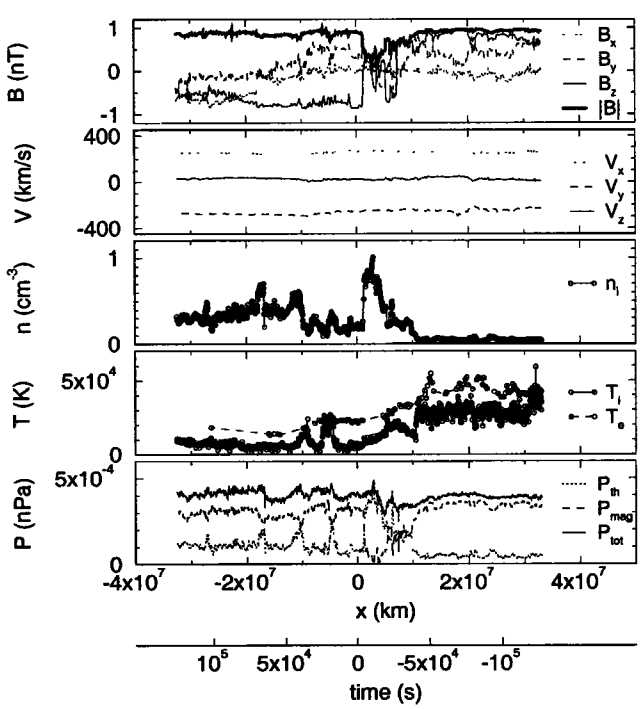

Figure 8. Context of the sector boundary observed by Ulysses on February 27, 1998. Magnetic field and solar wind velocity are shown in the minimum variance frame. The horizontal axes give the time elapsed since observation of the center of the structure and the corresponding distance.

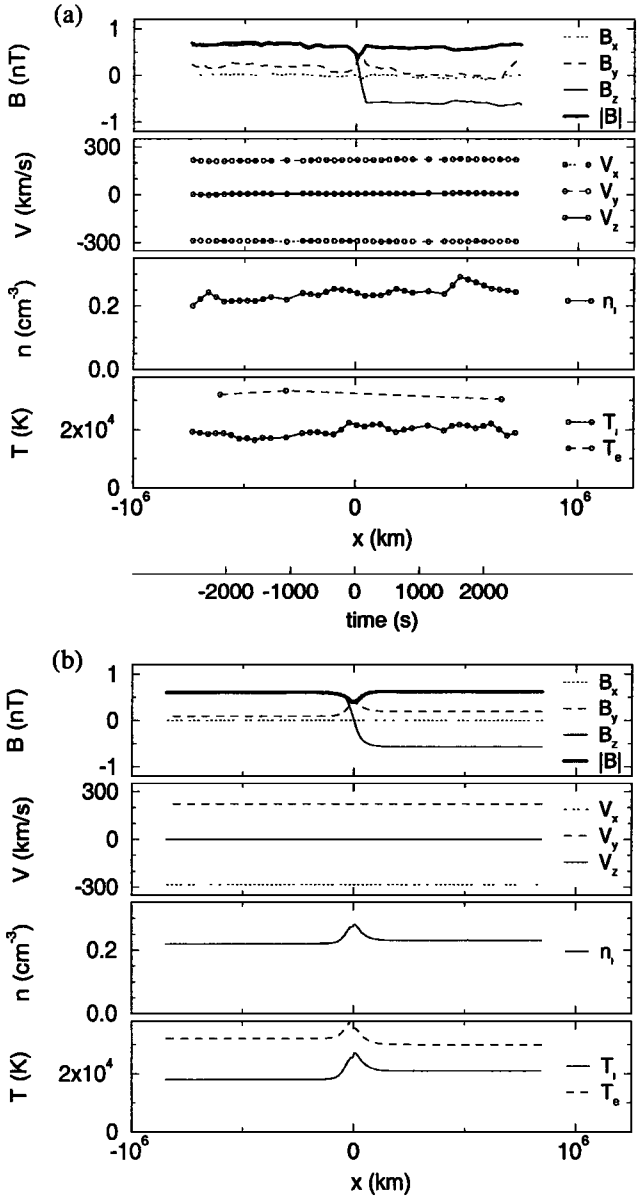

Figure 9. Sector boundary observed by Ulysses on February 27, 1998. (a) Ulysses observations in the minimum variance frame; the horizontal axes give the time elapsed since observation of the center of the structure and the corresponding distance. (b) Simulation assuming drifting protons and electrons trapped in the current layer.

rection. In the present example, the true current sheet thickness would be <100 gyroradii, an order of magnitude less than its apparent width. Convection of such a static wavy structure across the spacecraft may be the main cause for the observed ULF fluctuations. These have frequencies below 0.1 Hz, corresponding to ripple wavelengths above 10 ion gyroradii. The ripple wavelength therefore is on the order of the current sheet thickness.

6. Conclusions

We have studied sector boundaries observed by Ulysses at aphelion (5.4 AU), when it was nearly radially aligned with Wind at 1 AU. A direct comparison of Wind and Ulysses data is not easy. A hydrodynamic simulation helps to relate corresponding observations of interaction regions. It indicates where dynamic solar wind evolution is important, but it fails to correctly predict this evolution as it does not account for the proper geometry and as it neglects the role of the magnetic field. Starting from the sector structure observed at 1 AU, it predicts sector boundary location at 5 AU reasonably well except in the presence of strong transient

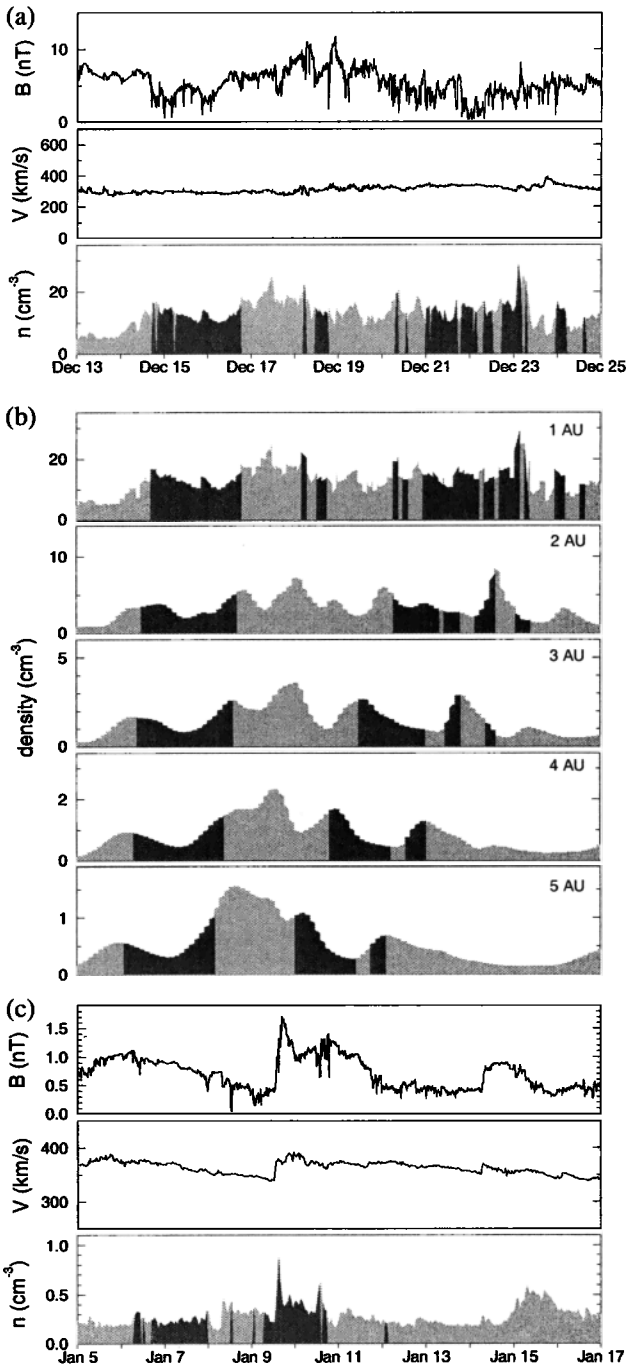

Figure 10. Solar wind evolution from 1 to 5 AU. (a) Wind observations at 1 AU. (b) Hydrodynamic simulation between 1 and 5 AU. (c) Ulysses observations at 5 AU. Light gray shading indicates inward magnetic field polarity; dark shading indicates outward polarity.

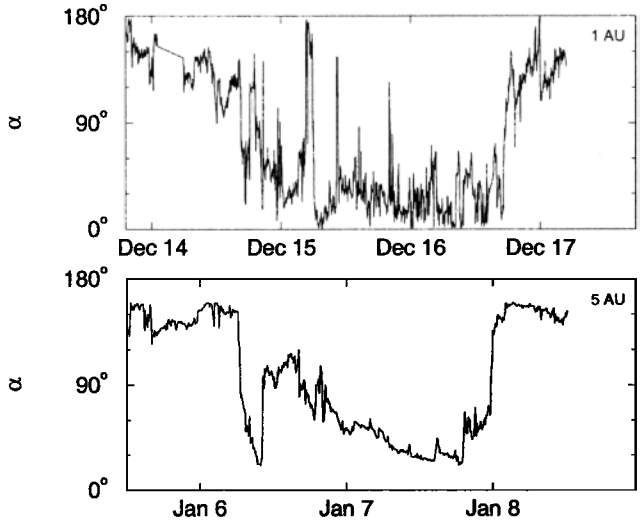

Figure 11. Comparison of the magnetic field observed by Wind (1 AU) and Ulysses (5 AU). In order to allow a comparison that is independent of the changing spiral angle and the magnetic field magnitude, we plot the angle α between the magnetic field vector and the outward Parker spiral direction.

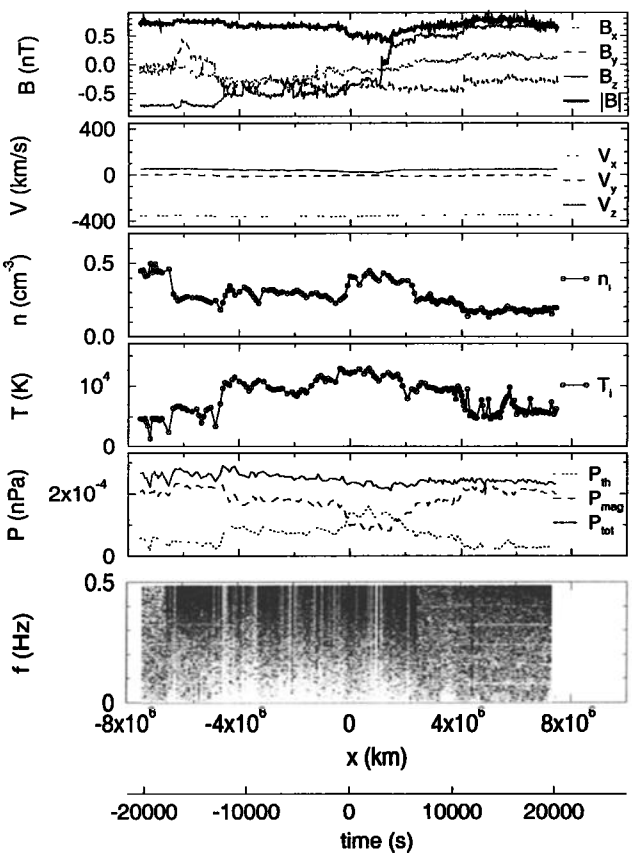

Figure 12. Context of the sector boundary observed by Ulysses on January 7–8, 1998. Magnetic field and solar wind velocity are shown in the minimum variance frame. The bottom plot shows the power spectral density of B_T (main transition component). The horizontal axes give the time elapsed since observation of the center of the structure and the corresponding distance.

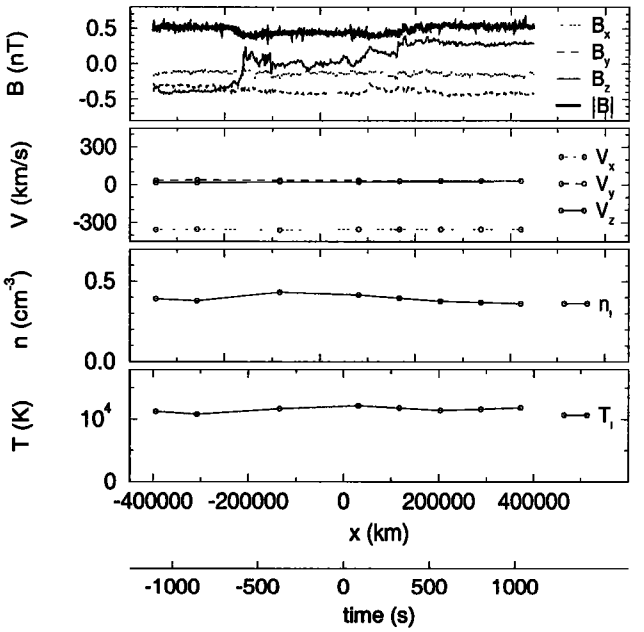

Figure 13. Sector boundary observed by Ulysses on January 7–8, 1998. Magnetic field and solar wind velocity are shown in the minimum variance frame. The horizontal axes give the time elapsed since observation of the center of the structure and the corresponding distance.

phenomena. While we observe a general similarity in se tor structure between 5 and 1 AU, the good correspondence between 1 AU sector boundaries and source surface predictions of the neutral line has been established before [*Burton et al.*, 1994; *Lepping et al.*, 1996]. The sector structure in the entire inner heliosphere therefore is well correlated with the coronal field during this period of low to modest solar activity. A similar conclusion regarding the macroscale coherence of the heliospheric current sheet was reached by *Siscoe and Intriligator* [1994] from a Pioneer 10 and 11 radial alignment study of the correlation between SBs observed by both spacecraft (at heliocentric distances of 1 and 2 AU).

For most Ulysses sector boundaries we were able to identify a corresponding Wind SB. Although the solar wind evolves considerably between 1 and 5 AU, and in spite of the change of the Parker spiral angle from 45° to 80°, we observe strong similarities in the large-scale appearance of these SBs (multiplicity, partial reentries in the current sheet): The undulating character of the heliospheric current sheet remains largely unchanged. In some cases we did not find a corresponding 1 AU sector boundary, but a magnetic cloud structure with nonspiral magnetic field. The interaction between the HCS and coronal transients has been discussed, for instance, by *Burton et al.* [1994], *Odstrčil and Pizzo* [1999a, b], and *Wu et al.* [1999].

The Ulysses SBs are embedded in a high-beta heliospheric plasma sheet, characterized by pressure balance as at 1 AU [*Winterhalter et al.*, 1994]. This is consistent with the view that the HCS is the contact surface between winds of different origin so that it often has the nature of a tangential

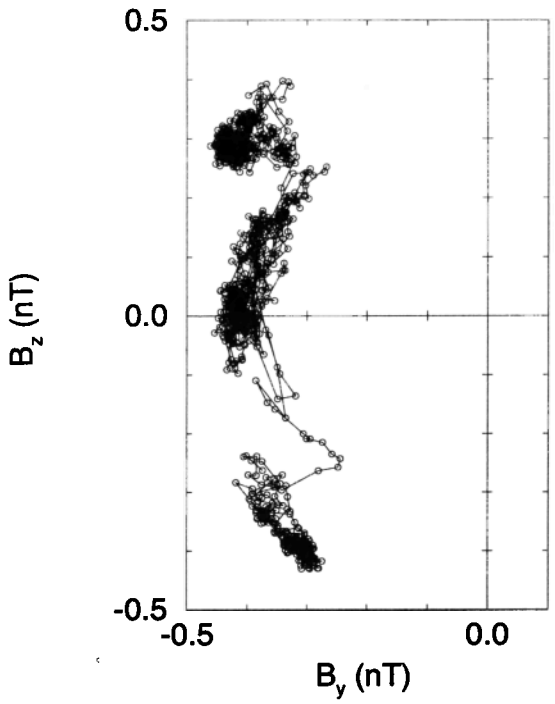

Figure 14. Hodogram of the tangential magnetic field components (in the minimum variance frame) for the sector boundary observed by Ulysses on January 7–8, 1998.

discontinuity. Minor pressure differences in the HPS have been washed out by the time the solar wind reaches 5 AU.

Inside the HPS we find the HCS. The main part of the transition typically is <100 ion gyroradii wide, although the full transition has a thickness that is an order of magnitude larger. Considerations of current sheet geometry and, in particular, of the nonplanar nature of the sheet indicate that the largest scales may be only apparent thicknesses. The true HPS and HCS thicknesses may be substantially smaller. The fact that the magnetic field vector in nonmonotonous polarity reversals traces essentially a single curve in the tangential magnetic field hodogram supports the concept of a rippled HCS. This concept was originally advanced by *Behannon et al.* [1981] in order to explain the observation of multiple, closely spaced HCS crossings. *Suess et al.* [1995] have developed a kinematic description of the deformation of the HCS due to radial velocity fluctuations at the base of the solar wind, over small spatial scales (corresponding to the size of supergranules on the Sun). They find that such fluctuations could be responsible for the observed solar wind flow inhomogeneities near the HCS, which would result in a "ruffling" of the HCS. Calculations by *Wang et al.* [1988] show that the sheared flow configuration near the HCS can excite kink mode instabilities; ripples in the HCS could be identified with such kink waves. The presence of ripples, in combination with geometrical effects, can explain much of the observed variability in sector boundary appearance and width. A rippled geometry (see Figure 15) is also consistent with the more or less radially outward direction of MVF normals for the HCS at 5 AU (see the discussion of HCS inclination with distance in section 2). A multiple-current-sheet sandwich structure can in general not be excluded [*Crooker et al.*, 1993, 1996], but such a structure cannot account for the properties of the magnetic field hodogram in at least one of the SBs studied here. Multisatellite observations could further enlighten these issues regarding curvature and multiplicity of the HCS.

Even accounting for a curved geometry, HCS thickness (tens of ion gyroradii to 100 ion gyroradii) remains typically larger than that of general solar wind TDs (1–30 gyroradii [e.g., *Burlaga et al.*, 1977]). SBs are a particular TD population characterized by large magnetic field rotations. The small-scale structure of the Ulysses SBs exhibits magnetic field depressions like at 1 AU [*Klein and Burlaga*, 1980; *Lepping et al.*, 1996]. Similar magnetic field depressions and density enhancements have been observed at the high-shear dayside magnetopause as well [*Hubert et al.*, 1998]. We have associated these depressions with drifting ions and electrons inside the TD layer that produce the net current required for the rotation of the magnetic field [*Harris*, 1962]. The limited plasma data time resolution available on Ulysses did not allow us to study this fine structure in more detail.

The tangential magnetic field in the HPS and HCS layers implies that particles are confined or trapped in these structures: The particles move parallel to the layer. The similarity between 1 and 5 AU sector boundary structure indicates that the overall shape of the HCS is conserved while the solar wind expands. No major instability seems to develop, which would obscure the similarity. This is supported by the observation that the velocity shear across the HCS or HPS does not exceed the thermal ion velocity, allowing TD equilibria to exist [see *De Keyser et al.*, 1997]. As the HCS structure seems to persist, the origin of the trapped particles must be sought closer to the Sun. Because of the correspondence with source surface maps we expect this trapping to take

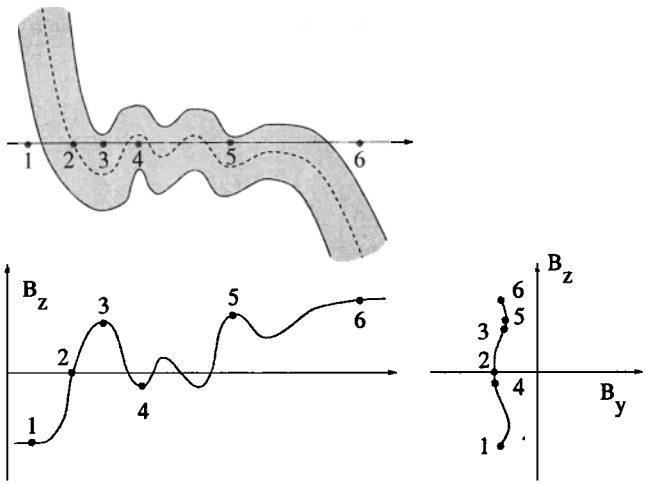

Figure 15. Crossing of a folded current sheet and its appearance in the minimum variance frame. The MVF normal points in the flow direction. The true thickness of the current sheet is much less than its apparent width. The tangential magnetic field components trace a single curve in the B_y-B_z hodogram.

place within the source surface, that is, inside the corona. This is supported by the often observed double ion beams near the HCS, which have been related to a coronal origin as well [*Hammond et al.*, 1995]. Once formed, the HCS structure changes in a quasi-static manner on its journey outward into interplanetary space.

Acknowledgments. This work was initiated at the Ulysses Aphelion Workshop, held on October 27–30, 1998, in Oxnard, California. We thank the PIs for the Wind MFI and SWE experiments, R. Lepping and K. Ogilvie. The work was performed at the Belgian Institute for Space Aeronomy under a PRODEX contract with ESA in the framework of the Ulysses Interdisciplinary Study on Directional Discontinuities. J.D.K. acknowledges the support of the Belgian Federal Services for Scientific, Technical and Cultural Affairs.

Michel Blanc thanks both referees for their assistance in evaluating this paper.

References

Behannon, K. W., F. M. Neubauer, and H. Barnstorf, Fine-scale characteristics of interplanetary sector boundaries, *J. Geophys. Res., 86,* 3273–3287, 1981.

Burlaga, L. F., J. F. Lemaire, and J. M. Turner, Interplanetary current sheets at 1 AU, *J. Geophys. Res., 82,* 3191–3200, 1977.

Burton, M. E., N. U. Crooker, G. L. Siscoe, and E. J. Smith, A test of source-surface model predictions of heliospheric current sheet inclination, *J. Geophys. Res., 99,* 1–9, 1994.

Crooker, N. U., G. L. Siscoe, S. Shodhan, D. F. Webb, J. T. Gosling, and E. J. Smith, Multiple heliospheric current sheets and coronal streamer belt dynamics, *J. Geophys. Res., 98,* 9371–9381, 1993.

Crooker, N. U., M. E. Burton, J. L. Phillips, E. J. Smith, and A. Balogh, Heliospheric plasma sheets as small-scale transients, *J. Geophys. Res., 101,* 2467–2474, 1996.

De Keyser, J., M. Roth, B.T. Tsurutani, C.M. Ho, and J.L. Phillips, Solar wind velocity jumps across tangential discontinuities: Ulysses observations and kinetic interpretation, *Astron. Astrophys., 321,* 945–959, 1997.

Forsyth, R. J., A. Balogh, T. S. Horbury, G. Erdös, E. J. Smith, and M. E. Burton, The heliospheric magnetic field at solar minimum: Ulysses observations from pole to pole, *Astron. Astrophys., 316,* 287–295, 1996.

Goldstein, B. E., M. Neugebauer, J. L. Phillips, S. Bame, J. T. Gosling, D. McComas, Y.-M. Wang, N. R. Sheeley, and S. T. Suess, Ulysses plasma parameters: Latitudinal, radial, and temporal variations, *Astron. Astrophys., 316,* 296–303, 1996.

González-Esparza, J. A., and E. J. Smith, Three-dimensional nature of interaction regions, Pioneer, Voyager, and Ulysses solar cycle variations from 1 to 5 AU, *J. Geophys. Res., 102,* 9781–9792, 1997.

Hammond, C. M., W. C. Feldman, J. L. Phillips, B. E. Goldstein, and A. Balogh, Solar wind double ion beams and the heliospheric current sheet, *J. Geophys. Res., 100,* 7881–7889, 1995.

Harris, E. G., On a plasma sheath separating regions of oppositely directed magnetic field, *Nuovo Cimento, 23,* 115–121, 1962.

Hubert, D., C. Harvey, M. Roth, and J. De Keyser, Electron density at the subsolar magnetopause for high magnetic shear: ISEE 1 and 2 observations, *J. Geophys. Res., 103,* 6685–6692, 1998.

Klein, L., and L. F. Burlaga, Interplanetary sector boundaries 1971–1973, *J. Geophys. Res., 85,* 2269–2276, 1980.

Lepping, R. P., A. Szabo, M. Peredo, and J. T. Hoeksema, Large-scale properties and solar connection of the heliospheric current and plasma sheets: WIND observations, *Geophys. Res. Lett., 23,* 1199–1202, 1996.

Odstrčil, D., and V. J. Pizzo, Three-dimensional propagation of coronal mass ejections (CMEs) in a structured solar wind flow, 1, CME launched within the streamer belt, *J. Geophys. Res., 104,* 483–492, 1999a.

Odstrčil, D., and V. J. Pizzo, Three-dimensional propagation of coronal mass ejections (CMEs) in a structured solar wind flow, 2, CME launched adjacent to the streamer belt, *J. Geophys. Res., 104,* 493–503, 1999b.

Pizzo, V. J., D. S. Intriligator, and G. L. Siscoe, Radial alignment simulation of solar wind streams observed by Pioneers 10 and 11 in 1974, *J. Geophys. Res., 100,* 12,251–12,260, 1995.

Roth, M., J. De Keyser, and M. M. Kuznetsova, Vlasov theory of the equilibrium structure of tangential discontinuities in space plasmas, *Space Sci. Rev., 76,* 251–317, 1996.

Siscoe, G., and D. Intriligator, Macroscale coherence of the heliospheric current sheet, Pioneers 10 and 11 comparisons, *Geophys. Res. Lett., 21,* 2075–2078, 1994.

Suess, S. T., and E. Hildner, Deformation of the heliospheric current sheet, *J. Geophys. Res., 90,* 9461–9468, 1985.

Suess, S. T., D. J. McComas, S. J. Bame, and B. E. Goldstein, Solar wind eddies and the heliospheric current sheet, *J. Geophys. Res., 100,* 12,261–12,273, 1995.

Svalgaard, L., J. M. Wilcox, P. H. Scherrer, and R. Howard, The Sun's magnetic sector structure, *Sol. Phys., 45,* 83–91, 1975.

Thomas, B. T., and E. J. Smith, The structure and dynamics of the heliospheric current sheet, *J. Geophys. Res., 86,* 11,105–11,110, 1981.

Villante, U., and R. Bruno, Structure of current sheets in the sector boundaries, Helios 2 observations during early 1976, *J. Geophys. Res., 87,* 607–612, 1982.

Wang, S., L. C. Lee, C. Q. Wei, and S.-I. Akasofu, A mechanism for the formation of plasmoids and kink waves in the heliospheric current sheet, *Sol. Phys., 117,* 157–169, 1988.

Wilcox, J. M., and N. F. Ness, Quasi-stationary corotating structure in the interplanetary medium, *J. Geophys. Res., 70,* 5793–5805, 1965.

Winterhalter, D., E. J. Smith, M. E. Burton, N. Murphy, and D. J. McComas, The heliospheric plasma sheet, *J. Geophys. Res., 99,* 6667–6680, 1994.

Wu, S. T., W. P. Guo, D. J. Michels, and L. F. Burlaga, MHD description of the dynamical relationships between a flux rope, streamer, coronal mass ejection, and magnetic cloud, An analysis of the January 1997 Sun-Earth connection event, *J. Geophys. Res., 104,* 14,789–14,801, 1999.

J. De Keyser and M. Roth, Belgian Institute for Space Aeronomy, Ringlaan 3, B-1180 Brussels, Belgium. (Johan.DeKeyser@bira-iasb.oma.be; Michel.Roth@bira-iasb.oma.be)

R. Forsyth, Space and Atmospheric Sciences, The Blackett Laboratory, Imperial College, Prince Consort Road, London SW7 2BZ, England, UK. (r.forsyth@ic.ac.uk)

D. Reisenfeld, Space and Atmospheric Sciences, P.O. Box 1663, MS D466, Los Alamos National Laboratory, Los Alamos, NM 87545. (dreisen@lanl.gov)

(Received July 19, 1999; revised March 1, 2000; accepted March 2, 2000.)